Design for Additive Manufacturing and Finite Element Analysis of Fe-Mn Biodegradable Fracture Fixation Plate with Varying Porosity Levels

Mustafiz Shaikh [a], Fadi Kahwash [a], Zhilun Lu [a], Mohammad Alkhreisat [b, c], *and Islam Shyha [a]*

a School of Computing, Engineering and the Built Environment, Edinburgh Napier University, Edinburgh EH10 5DT, UK
[b] MD, FRCS Trauma and Orthopaedic, Newcastle University Hospitals, UK
[c] Albalqa Applied University, Jordan

Abstract. Fracture fixation plates are osteosynthesis implants used to fix fractured bones in a human body. They are either left in the body or required to be removed after a bone healing period of 3-6 months. Recent trends focus on developing iron (Fe) based porous biodegradable implants eliminating the need for revision surgery. However, Fe alloys in their porous state are prone to a higher rate of corrosion resulting in detrimental mechanical properties. This study proposes a design strategy to develop fracture fixation implants mimicking natural cortical bone, i.e., targeting to possess enough structural strength with a minimal level of porosity. Three fixation plates each with 5, 10, and 15% porosity are developed having a gyroid lattice structure of Triply Periodic Minimal Surface designs. Four-point bending simulation is performed on Ansys to characterize the mechanical properties of the designed implants. Results show a decreasing trend of bending strength and flexural stiffness with higher porosity, but still relevant for fixation of fractured sites at different regions. The bending properties of developed implants are compared with USFDA's proposed performance criteria, which shows 5% porous implants capable of all load-bearing extremities, whereas implants having 10 and 15% porosity are deemed to be suitable for tibia and humerus fixation.

Keywords: Fracture fixation plate, design for additive manufacturing, four-point bending test simulation, metal additive manufacturing, triply periodic minimal surface design, porous implant.

1 INTRODUCTION

Osteosynthesis or Fracture fixation devices are a class of temporary implant used for fixing fractured bones in the human body. Fixation implants are of different types ranging from plates, screws, wires, intramedullary rods, and pins [1]. These devices are fixed in a manner that they support bone until the healing period, the major goal here is to direct load acting on a bone to these implants while the fractured bone is in a process of healing [2].

Depending on the type of fracture and complexities in terms of surrounding tissues, fixation implants are either left in the body or required to be removed with revision surgery. Haseeb et al [3] studied the post operative functioning of fracture fixation implants. Their study indicated pain and implant's structural prominence as the main reasons contributing to revision surgery for implant removal. Other than these two reasons, patient's insistence caused by discomfort and inability to perform certain routine functions due to limited freedom of mobility is the next common factor contributing to the need for revision surgery in fixation implants.

Commercially pure titanium, stainless steel and cobalt chromium alloys are conventional metals used for current fixation implants. These alloys possess high modulus of tensile elasticity triggering stress shielding effect which causes bone deterioration and implant loosening [4]. Due to the absorption in majority of stress by the metallic implants with high stiffness, adjacent bones are inhibited from their regular load bearing activity causing passivation which results in weaking of the bones [5]. Young's modulus for metallic alloys are usually 10 times higher than cortical bone. Polymers and their composites have been in research to overcome the ineffectiveness of high strength metals. High density polyethylene, polyamide, and polyether ether ketone are some polymers being investigated for fixation applications. These materials have Young's modulus matching or sometimes less than cortical bone, but they are still been proven to be safe for application in maxillofacial treatments, yet not suggested for load bearing extremities in tibia, femur and humerus bone [6].

The innate capability of metal additive manufacturing (MAM) to produce parts with layer-by-layer processing, has opened avenues to develop parts with controlled architecture and intricate features. Stainless steel and titanium based metallic implants having topologically optimized structures and porous lattices are investigated to reduce typical Young's modulus anticipating lowered effect of stress shielding. Erica et al. [7] studied the implication of developing Co-Cr implants with porous architecture having pore size of up to 1000 μm. Porous lattice structures in this study showed uniform distribution of loads to cortical bone, suggesting use of porous Co-Cr for implant with reduced stress shielding.

Although MAM has shown promising results in eliminating stress shielding with porous metallic alloys, research based on biodegradable implants is still in infancy. Bioresorbable fixation implant require nontoxic materials, which are biocompatible and have no harmful effects with degraded ions in physiological environment [8]. Biodegradable fixation devices have been developed and tested using polymeric and metallic materials. Where PLGA based pins and Magnezix screws are prime example [9, 10]. But applications of such materials for load bearing application like intramedullary rod and osteosynthesis plates is still a challenge as they are required to possess higher mechanical strength, where polymers have very low mechanical strength and Mg has very low resistance to corrosion.

Mg, Zn, and Ca based alloys are materials being researched for load bearing biodegradable implants, but these alloys have shown very high rate of corrosion, making them suitable only for scaffolding applications or in case of implants not requiring longevity. Erinc et al. [11] proposed that the required corrosion rate for osteosynthesis implants should be 0.5 mm $year^{-1}$, which can support fractured site for a 3-6 months of

bone healing period. Pure Fe and its alloys with Mn, Pd, Au, and Ag are currently being investigated as they present good biocompatibility for bone homeostasis and higher corrosion resistance than Mg. Although pure Fe shows a corrosion rate of 0.01 mm $year^{-1}$, its alloys with Mn have shown considerable rise in corrosion rate from 0.07 to 0.2 mm $year^{-1}$ [12].

Metallic alloys are required to possess a controlled rate of corrosion to be used for biodegradable implant application, it is the rate at which metal ions disintegrate in the biological environment. This factor invariably affects bone healing and structural prominence of the implants. Researchers have developed porous parts with Fe-35Mn which has further led to an increased corrosion rate of up to 2 mm $year^{-1}$ [13]. But this rate is too high to be used for fixation implants. Moreover, their mechanical properties are drastically low, making them applicable only for scaffolding of cancellous bones [14].

This study proposes a strategy of bio mimicking to develop Fe-35Mn based fixation implants with minimal porosity levels in the range of 5 to 15% matching natural cortical bone [15]. Triply Periodic Minimal Surface (TPMS) lattices are used to produce porous structures. Inducing porosity results in drastic decrease of mechanical properties in Fe based biodegradable implants. Therefore, this study primarily emphasizes analyzing bending characteristics of newly designed fracture fixation implant. Four-point bending simulation is executed on Ansys to compare performance of porous implants under investigation.

2 INVESTIGATIONAL METHODOLOGY

2.1 Bending Strength Characterization

Open reduction internal fixation (ORIF) is where osteosynthesis plates are used in cases where the bones are fractured in a way that they are displaced from their usual line of axis. Plates, Pins, and Screws are used to hold damaged bone in its natural state of alignment during the time it heals. Bones like femur, tibia and humerus in their natural state are not linearly straight having convex and concave sides [16] . In typical loading conditions, the concave side of bone experiences compressive forces, while convex side is under tensile load. In case of fracture, convex side is susceptible to expansion due to tensile forces, while compressive forces on concave side close the fracture.

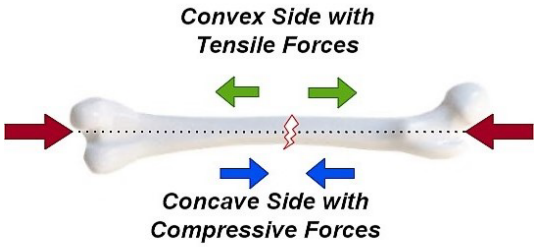

(A) Fracture Gap Without Fixation Implant

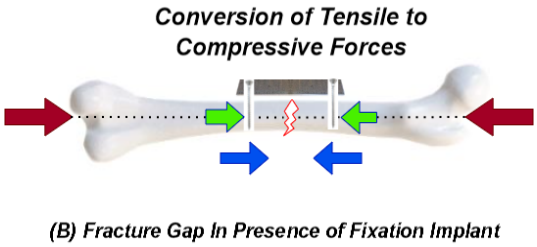

Fig. 1. Tensile Band Principle

Following the principle of tensile band, fixation plates are screwed on the convex side of the bone, converting tensile forces to compressive forces in the open fracture [17]. This condition makes the fixation plate susceptible to bending moment, therefore, ASTM (American Society for Testing and Materials) and USFDA (United States Food and Drug Administration) recommend a standard four-point bending test to assess performance criteria for the clinical fracture fixation plates. Fig. 1 represents loading condition, and tensile band principle for facture fixation.

Finite Element Analysis (FEA) with static four-point bending configuration is performed in this study to characterize mechanical properties of the proposed implants. ASTM F-382 is standard which defines bending strength, proof load, bending stiffness and equivalent structural stiffness as criteria to characterize bending properties of metallic fracture fixation plate subjected to bending forces [18]. Fig.2 shows the generic loading configuration used in this setup and calculation method of drafting yield point in load vs deformation curve. The following sections shows the testing method used to characterize each bending property of fixation plates, subjected to static four-point loading system:

1. [Bending Stiffness - K] (N/mm), is bone plate's resistance to deformation against bending loads. It is calculated by determining slope of a straight line (OM) for elastic region of load vs deformation curve. It is a factor depending on material under study and the fixation plate's geometry.
2. [Proof Load] (N) is the yield point where, fixation plate under study is susceptible to a 0.2% offset displacement. This region is an intersecting point, where load vs displacement curve meets the offset line (BC). Offset distance for drafting the line BC is a function of loading setup defined by,

$$Offset\ Distance\ OB = 0.002\ (a) \qquad (1)$$

Were, a is the center span distance between internal loading pins.

3. [Equivalent Structural Stiffness – EI_e] (Nm^2) is the normalized stiffness considering effect of test configuration setup. It is measured as follows,

$$EI_e = \frac{(2h+3a)Kh^2}{12} \qquad (2)$$

Were,
h is the distance between loading and supporting pins,
a is the centre span distance between internal loading pins, and
K is the Bending stiffness.

4. [Bending Strength] (N-m), is the moment required to cause an offset displacement in the fixation plate. It is calculated as follows,

$$\text{Bending Strength} = \frac{P(h)}{2} \qquad (3)$$

were, P is the proof load and h is the distance between external support pins.

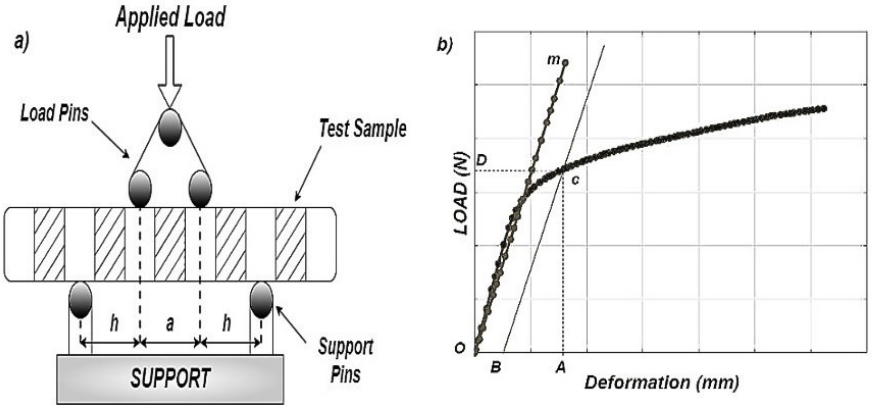

Fig. 2. (a) ASTM F382 Four Point Bending Setup and (b) Estimation of Proof Load [18]

2.2 Preparation of FEA Model

Setup Configuration. A static structural four-point bending simulation was conducted on Ansys workbench. Fig.3 shows the system structure used in this simulation. It was arranged to duplicate standard ASTM F382 bending setup [18]. The loading configuration comprised of pin A, B, and C in a joint boundary condition. Load was applied with increments through pin A in vertical direction, where B and C acted as supported loading pins. This configuration was free to move along vertical axis and constrained through their respective lateral direction in X and Z axis. Fixed supported pins D and E were constrained in all directions. No constraints were applied directly on fixation plate, but a frictional connection was maintained through pins B, and C with a 0.3 coefficient of friction. Where a frictionless connection was retained with fixed supported pins D and E. Radius of each roller was 5 mm, and distance a and h were maintained such that the pins were not in direct contact with screw holes. These conditions were maintained with adherence to similar trend followed by Liao et al. [19].

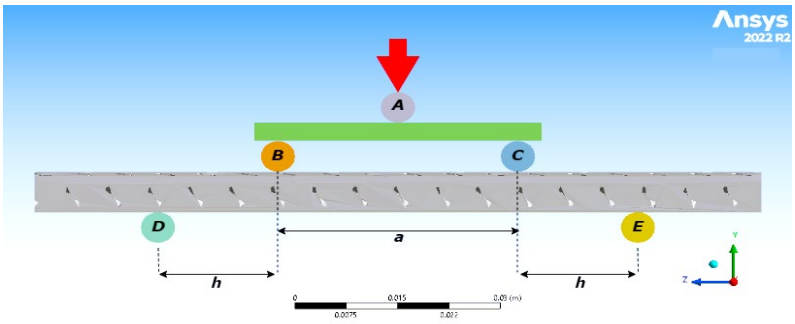

Fig. 3. Four-Point Bending Setup in Ansys Workbench

Model Validation. Two-stage validation was performed to verify this model for simulation of porous implants. Experimental data from two previous studies performed on fixation implants of different geometry were selected. The calculated bending characteristics were compared to experimental investigations of Liao et al. [19], and Lee et al. [20]. They performed a four-point bending simulation on an CpTi (Commercially pure Titanium) based 8-hole LC-DCP (Limited Contact Dynamic Compression Plate), and a 9-hole tibial fixation plate respectively. Table 1 defines setup parameters used in the simulation. An optimal mesh size of 1 mm was used in this study after performing a mesh independence study.

Table 1. Setup Configuration for Bending Simulation

Implant Type	Material	Implant Thickness (mm)	Rate of Applied Load (mm/min)	Distance between Pins (mm)	
				a	h
LC-DCP	CpTi	3.3	3	28	26
Tibial	CpTi	4.5	5	35	17.5
Porous	Fe35Mn	5	5	35	17.5

Material properties, geometry, and device setup were mimicked in accordance with the experimental study in comparison. Primarily simulation was performed for a 3.3 mm thick CpTi fixation implant having 8 holes, followed by a validation for 4.5 mm thick CpTi implant with 9 holes. Multi-linear Isotropic hardening model was used to fully capture the material plasticity. Engineering stress and strain values were extracted for CpTi, and Fe-35Mn with reference to the available tensile test data [21, 22]. Post validation, the verified model was further used to analyze bending properties of porous fracture fixation implants. Table 2 shows material properties used for this simulation.

Table 2. Physical and Elastic Properties of Materials under Study

Alloy System	Density (kg/m^3)	Young's Modulus (Gpa)	Poisson's Ratio
CpTi	4591	110	0.37
Fe-35Mn	7630	179	0.3

2.3 Formulation of Porous Design

N-topology software was used to develop porous fracture fixation implant in this research. Employing the concept of biomimetics, fracture fixation plates were designed having similar level of porosity to a cortical bone. Three designs having a lattice induced porosity of 5, 10 and 15% were created using gyroid based TPMS cells. Gyroid structures are convex, and concave combinations of non-intersecting surfaces. Formation of a gyroid based 3D structure is sine, cosine function in a three-dimensional cartesian coordinate. Equation (4) represents, governing function of TPMS gyroid cell.

$$F\ (x, y, z) = cos(x) \cdot sin(y) + co\,s(y) \cdot si\,n(z) + co\,s(z) \cdot si\,n(x) + C \quad (4)$$

In the above equation, C is control function determining offset between gyroid surface, which affects the percentage of part porosity. When C=0, the gyroid surfaces divides domain into two equal regions of void and solid, forming a 50% porous space. Similarly ranging the values from -1.5, 0 and +1.5 provides control of part porosity in a gyroid unit cell. Walker et al. [23] devised an algorithm to develop gyroid based porous structures with user defined pore size, strut size, and percentage of porosity. Fig.4 represents a relationship between level constant C, porosity, and pore/strut ratio from their study. A polynomial fit with an R^2 value of 1.000, gives a direct relation between level constant C and porosity (n).

$$C = 0.7864n^3 - 1.1798n^2 - 2.5259n + 1.4597 \quad (5)$$

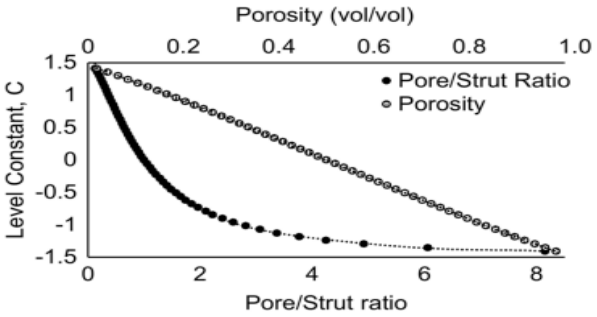

Fig. 4. Relation between level constant C, Pore/Strut Ratio, and Porosity

Using equation (5) and the requirement to mimic cortical bone porosity, level constants values were determined for achieving 5, 10 and 15% of porosity. Porous fracture fixation implants were developed by performing Boolean intersection of gyroid cells in the volumetric space of base design. The fracture fixation device used in this study is a 5mm thick femoral fixation plate with 6 holes for 4.5 mm cortical screws. Design information for fixation implant is acquired from TIPSAN® design data sheet [24]. Fig.5 represent design methodology followed for developing porous designs using N-topology.

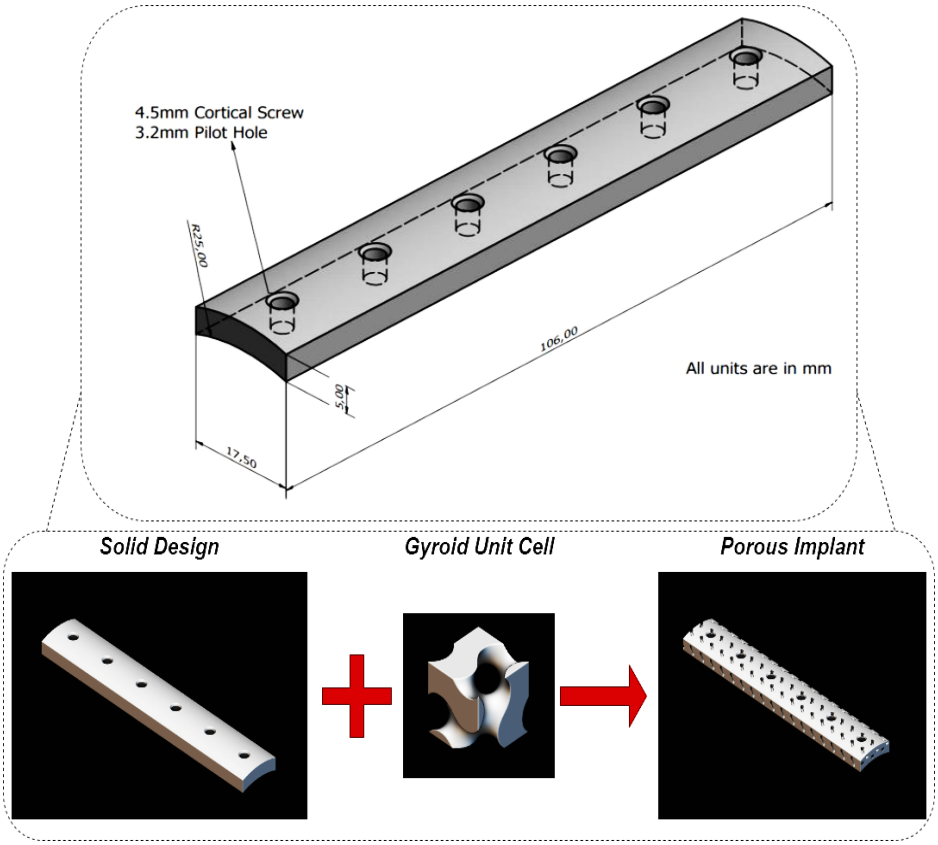

Fig. 5. Design Specification of Porous Fixation Implant

The primal implant model developed in this investigation through N-topology is an implicit body representing Boolean intersection of gyroid cells to mapped solid design of implant. The implicit body was further re meshed with simplification, followed by reduction in number of faces to be used for simulation. Fig.6 signifies end fixation plate developed with reduced number of faces. To verify competency of developed model, the end design's mass and volume estimation were compared to values of non-porous solid implant model. Table 3 shows the relevant reduction of mass and volume values to the similar level of target porosity to be achieved by the design.

Table 3. Implant Design Porosity Validation

Solid Implant	Target Porosity %	Level Constant	Mass (gm)	Volume (mm^3)	Reduction %
Mass 71.99 gm	5	1.330	68.39	8571	5
	10	1.196	64.85	8123	10
Volume 9021 mm^3	15	1.056	61.38	7685	15

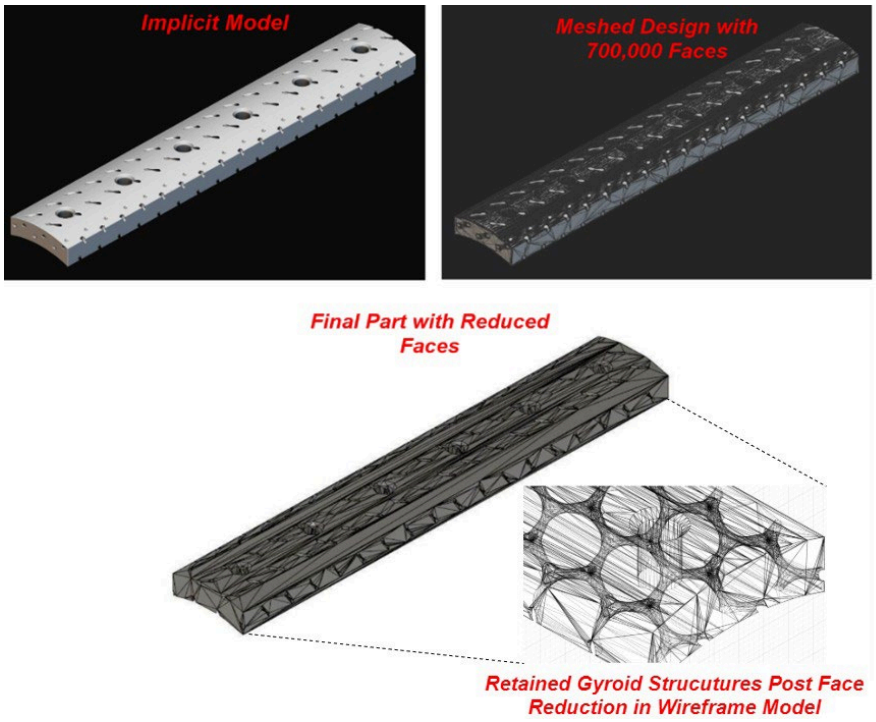

Fig. 6. Design Simplification for Feasible Simulation

3 RESULTS AND DISCUSSIONS

3.1 Proposed Model Validation

FEA based four-point bending investigation was performed with validation to experimental analysis of fracture fixation implants with different dimensions i.e., a 3.3 mm LC-DCP implant with 8 holes and 4.5 mm Tibial implant with 9 holes. Devised simulated model is validated for plates with different dimensions to ensure geometrical dependency. This way the model is authenticated to be used for fixation implants designed in this study with varied pore size and lattice structures. Simulated results showed reliance on implants dimensions like thickness and functional features like hole. These factors should thus be considered carefully while developing a new fixation device. The developed bending simulation model under study shows a marginal variation to experimental data. In overall comparison, both models showed 98 to 99% similarity in calculation of proof load and bending strength. Fig.7 shows a comparison in variance of load vs deformation curve for experimental and simulated data for the two fixation implants under study. Both simulations show similar trend to experimental data, where both graphs present noticeably comparable linear elastic region and yield point, which is proven by apparent similarity in calculated values of proof load and bending strength.

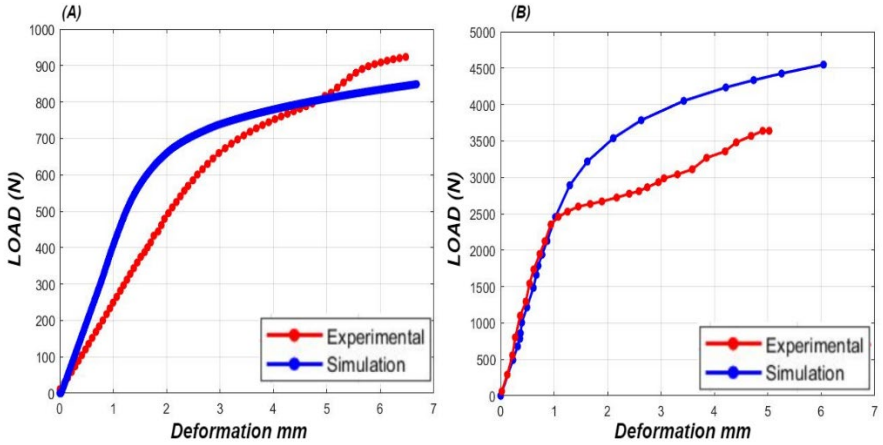

Fig. 7. Load vs Deformation Curve for A) LC-DCP and B) Tibial Fixation Implant [19], [20]

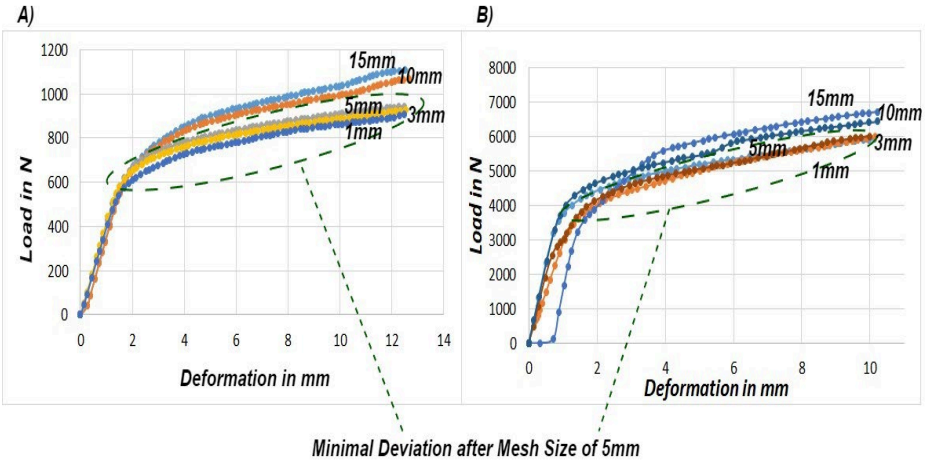

Fig. 8. Mesh Convergence Analysis with Element Size of 15,10,5,3, and 1 mm A) LC-DCP and B) Tibial Fixation Implant

Discussion on Reported Values. In overall comparison the simulated model showed promising similarity to experimental data. The maximum level of variance was noted in 3.3mm LC-DCP implant with 35% increase in structural stiffness. Stiffness properties are evident dimension dependent property, this increase could be an effect of incompetent reproduction of design dimensions to experimental study. Fig.8 signifies a mesh convergence analysis performed to match experimental stiffness values, study was conducted with mesh size ranging from 15 to 1 mm, which showed no considerable difference in calculated data after a 5mm element size. Also, a comparative analysis with different plasticity models of bilinear and multi-linear isotropic hardening were compared, showing no convincing difference in stiffness values. Fig.9 represents a comparison in experimental and calculated data from simulations.

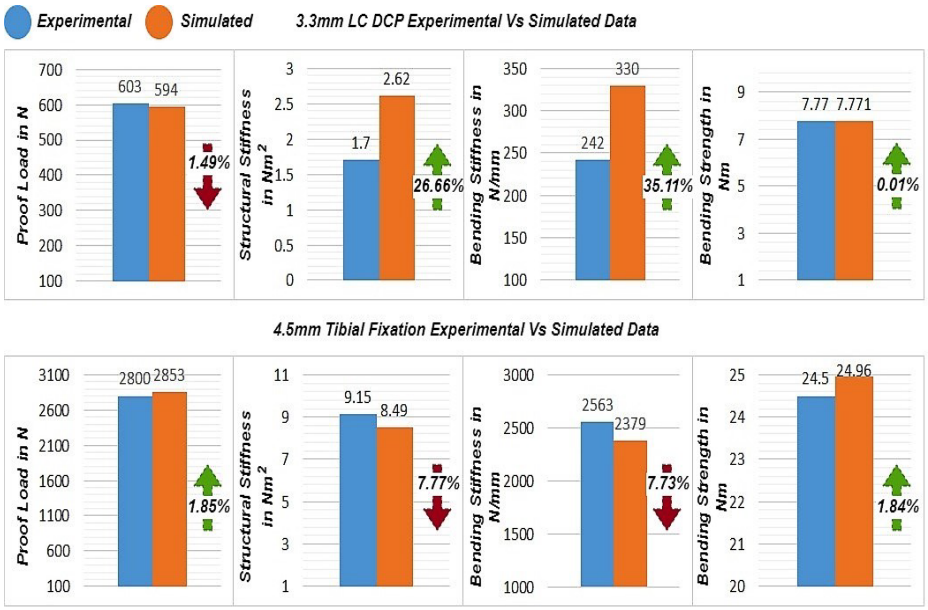

Fig. 9. Experimental and Simulated Bending Properties for Fully Solid 3.3mm LC DCP and 4.5mm Tibial Fixation Implants [19], [20]

Although the simulated model of LC-DCP showed an increase in calculated stiffness values, it is still well competent with its proof load and bending strength calculation having at most similarity to experimental data. Moreover, simulation of 4.5mm tibial fixation implant showed promising results with bending property values exactly similar to experimental data. A variation in a range of -7.77% to 1.84% was recorded, which shows an impressive reliance for the simulated model.

3.2 Bending Strength Analysis of Proposed Design

Simulations for design with Fe-35Mn alloy was performed in two stages, initially with fully dense model, followed by designs having lattice induced porosity. All porous samples showed substantial feasibility under bending loads, where fully dense designs had the highest flexural stiffness and bending strength. This trend is anticipated, but the main goal is to induce porosity without causing detrimental decrease in mechanical properties, which is achieved by this proposed route of architected porous design.

Table 4. Effect of Porosity on Stress and Deformation Properties

Type of Implant	*Stress Generation MPa*	*Max Deformation mm*
Dense	658	9.5
5% Porosity	710	15
10% Porosity	713	15
15% Porosity	715	15

Table 4 shows the difference in stress generation and total deformation values for different designs. Evident trend in increasing range of equivalent von mises stress generation is recorded for designs with rising levels of porosity.

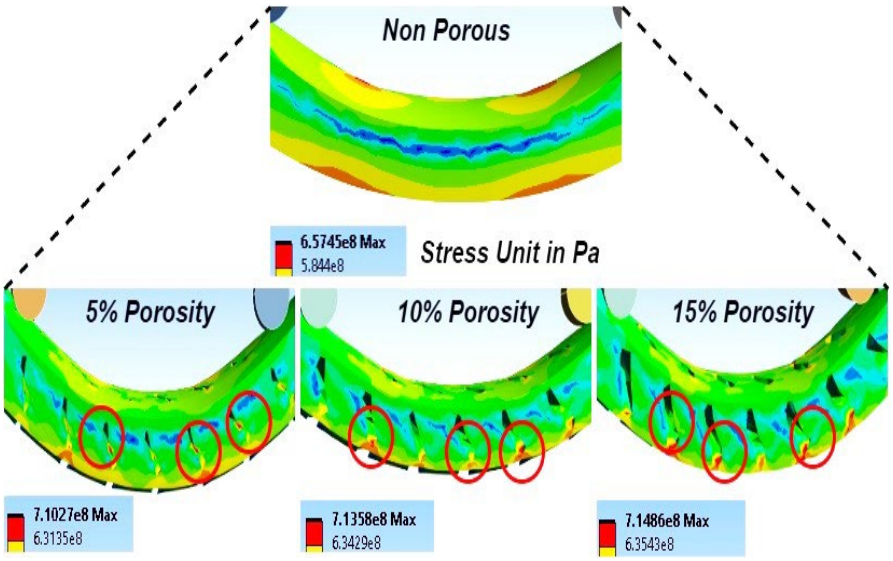

Fig. 10. Difference in Stress Concentration Regions between Non-Porous and Porous Designs

Fig.10 signifies distribution of stress levels for different designs of implant in their highest state of deformation under study. Nonporous implants have higher points of stress developing at their posterior side subjected to extensive tension, and at circumference of screw holes. Highest level of stress recorded is 658 MPa at 9.5 mm deformation. While a higher rate of deformation reaching maximum of 15mm with stress values of 710, 713, and 715 MPa are recorded for 5, 10 and 15% porous implants respectively. This increasing trend of detrimental mechanical properties is attributed to increase in pore induced stress concentrations. Fig.10 can also be appreciated to look at increase in stress concentration points induced by porosity.

Table 5. Comparison of Bending Properties of Porous Implants to USFDA Performance Criteria

Intended Anatomical Site		Bending Strength Nm	Structural Stiffness Nm^2	Porosity %		
				5	10	15
Upper Extremity	Humerus	10.44	3.96	✓	✓	✓
Lower Extremity	Femur/ Proximal Tibia	23.67	7.8	✓	×	×
	Distal Tibia	10.53	3.15	✓	✓	✓

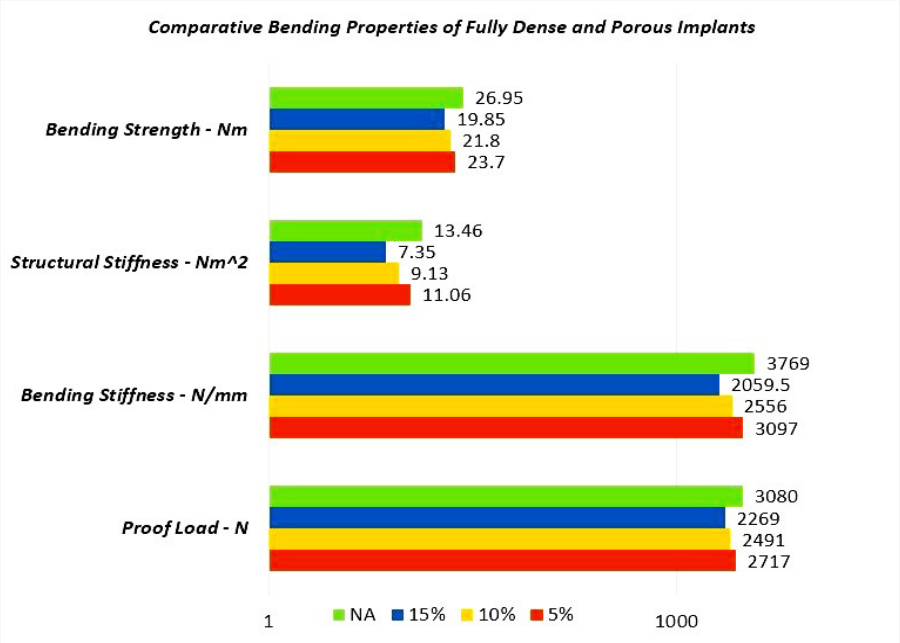

Fig. 11. Comparative Bending Properties of Porous and Fully Dense Fe-35Mn Fixation Implant

Bending strength characteristics for dense Fe-35Mn showed their competency to be used for possible application in femoral fixation and other lower and upper proximities of human body. Fig.11 represents a comparative analysis on bending characteristics of porous and fully dense implants. Although results show substantial capability to use dense Fe-35Mn for femoral fixation, their porous counterparts reveal decreasing trend of bending properties. Applicability of designed implants is judged with comparison to a performance criterion proposed by USFDA for fixation implants in different proximities of body. Table 5 represents different performance criteria for fixation implants and the appropriate regions where the developed porous implants could be used [25].

4 CONCLUSIONS

Porous Fe-35Mn with its capacity to degrade has been investigated by earlier researchers for bioabsorbable osteosynthesis implants. But inducing porosity has always been reported with detrimental decrease in mechanical properties making them suitable only for non-load bearing applications like stents and pins. In this research, a novel route of biomimetic involving development of fracture fixation implant with minimal levels of porosity matching cortical bone has been introduced and analyzed for their bending strength characteristics. The following conclusions can be drawn from this study:

- Experimental validation showed similarity to all calculated bending properties for 4.5 mm tibial implant, but an increase in stiffness values were observed for the 3.3

mm LC-DCP implant, a further refinement of this model can be performed. Involvement of material damage model will further improve the approximation.

- Minimal porosity implants have shown promising applications for the development of biodegradable fracture fixation device. Plates with highest level of porosity of 15% showed lowest strength of order 19.85 Nm, and equivalent stiffness of 7.35 Nm^2, which is below the criteria for femoral fixation but still relevant for other proximities like tibial, and humerus fixation.
- 5% porous fixation implants with 23.7 Nm of bending strength and equivalent stiffness of 11.06 Nm^2 meet the performance criteria of USDFA for femoral fracture fixation.
- Further research is required to deduce biodegradability aspect of designed implant, inducing porosity would have increased their rate of corrosion exceeding 0.07 mm $year^{-1}$. A corrosion rate equal or under 0.5 mm $year^{-1}$ is ideal for fracture fixation device.
- An attempt has been made to characterize primitive mechanical properties of designed implants. Further analysis on sharp corroding structures and their effects on strength of these components will additionally support the claims of this study.
- Mechanical and corrosive properties can be further increased by alloying the Fe-35Mn alloy system with other biocompatible elements. Process induced microstructural enhancement such as heat treatment can also increase their mechanical properties.
- Layer by layer additive manufacturing is believed to be the best processing technique that can manufacture the proposed TPMS structures retaining the target percentage of porosity. A study on MAM of proposed design with post process mechanical and corrosion analysis will advance this research in development of first in practice biodegradable load bearing fixation plates.

References

1. Kim T, See CW, Li X, Zhu D (2020) Orthopedic implants and devices for bone fractures and defects: Past, present and perspective. Engineered Regeneration 1:6–18. https://doi.org/10.1016/j.engreg.2020.05.003
2. Pankaj P (2022) Devices for traumatology: Biomechanics and design. In: Human Orthopaedic Biomechanics: Fundamentals, Devices and Applications. Elsevier, pp 459–484
3. Haseeb M, Butt MF, Altaf T, Muzaffar K, Gupta A, Jallu A. Indications of implant removal: A study of 83 cases. Int J Health Sci (Qassim). 2017 Jan-Mar;11(1):1-7. PMID: 28293156; PMCID: PMC5327671.
4. Li J, Qin L, Yang K, et al (2020) Materials evolution of bone plates for internal fixation of bone fractures: A review. J Mater Sci Technol 36:190–208
5. Zhao X, Jing W, Yun Z, et al (2021) An experimental study on stress-shielding effects of locked compression plates in fixing intact dog femur. J Orthop Surg Res 16
6. On SW, Cho SW, Byun SH, Yang BE (2020) Bioabsorbable osteofixation materials for maxillofacial bone surgery: A review on polymers and magnesium-based materials. Biomedicines 8
7. Liverani E, Rogati G, Pagani S, et al (2021) Mechanical interaction between additive-manufactured metal lattice structures and bone in compression: implications for stress shielding

of orthopaedic implants. J Mech Behav Biomed Mater 121:. https://doi.org/10.1016/j.jmbbm.2021.104608
8. Prakasam M, Locs J, Salma-Ancane K, et al (2017) Biodegradable materials and metallic implants-A review. J Funct Biomater 8
9. Biber R, Pauser J, Geßlein M, Bail HJ (2016) Magnesium-Based Absorbable Metal Screws for Intra-Articular Fracture Fixation. Case Rep Orthop 2016:1–4. https://doi.org/10.1155/2016/9673174
10. Sinikumpu JJ, Serlo W (2017) Biodegradable poly-L-lactide-co-glycolide copolymer pin fixation of a traumatic patellar osteochondral fragment in an 11-year-old child: A novel surgical approach. Exp Ther Med 13:242–246. https://doi.org/10.3892/etm.2016.3934
11. Erinc M, Sillekens WH, Mannens RGTM, Werkhoven RJ Applicability of existing magnesium alloys as biomedical implant materials
12. Zhang Q, Cao P (2015) Degradable porous Fe-35wt.%Mn produced via powder sintering from NH4HCO3 porogen. Mater Chem Phys 163:394–401. https://doi.org/10.1016/j.matchemphys.2015.07.056
13. Li Y, Jahr H, Lietaert K, et al (2018) Additively manufactured biodegradable porous iron. Acta Biomater 77:380–393. https://doi.org/10.1016/j.actbio.2018.07.011
14. Wegener B, Sichler A, Milz S, et al (2020) Development of a novel biodegradable porous iron-based implant for bone replacement. Sci Rep 10:. https://doi.org/10.1038/s41598-020-66289-y
15. Morgan EF, Unnikrisnan GU, Hussein AI (2018) Annual Review of Biomedical Engineering Bone Mechanical Properties in Healthy and Diseased States. https://doi.org/10.1146/annurev-bioeng-062117
16. Friis EA, DeCoster TA, Thomas JC (2017) Mechanical testing of fracture fixation devices. In: Mechanical Testing of Orthopaedic Implants. Elsevier
17. Hommel GJ, Lobrano C, Ogden AL, et al (2011) A quantitative analysis of tension band plating of the femur diaphysis. Arch Orthop Trauma Surg 131:1325–1330. https://doi.org/10.1007/s00402-011-1294-5
18. Standard Specification and Test Method for Metallic Bone Plates 1, Standard Specification and Test Method for Metallic Bone Plates (astm.org)
19. Liao B, Sun J, Xu C, et al (2021) A mechanical study of personalised Ti6Al4V tibial fracture fixation plates with grooved surface by finite element analysis. Biosurf Biotribol 7:142–153. https://doi.org/10.1049/bsb2.12019
20. Lee S, Ahmad N, Corriveau K, et al (2022) Bending properties of additively manufactured commercially pure titanium (CPTi) limited contact dynamic compression plate (LC-DCP) constructs: Effect of surface treatment. J Mech Behav Biomed Mater 126:. https://doi.org/10.1016/j.jmbbm.2021.105042
21. Eid C, Martini FM, Bonardi A, et al (2017) Single cycle to failure in bending of three titanium polyaxial locking plates. Veterinary and Comparative Orthopaedics and Traumatology 30:172–177. https://doi.org/10.3415/VCOT-16-07-0111
22. Hermawan H, Dubé D, Mantovani D (2007) Development of degradable Fe-35Mn alloy for biomedical application. In: Advanced Materials Research. Trans Tech Publications, pp 107–112
23. Walker JM, Bodamer E, Kleinfehn A, et al (2017) Design and mechanical characterization of solid and highly porous 3D printed poly(propylene fumarate) scaffolds. Progress in Additive Manufacturing 2:99–108. https://doi.org/10.1007/s40964-017-0021-3
24. Broad Plate MC-DCP 4.5 mm, TIPSAN_Plate_Implants.pdf
25. Orthopedic Fracture Fixation Plates - Performance Criteria for Safety and Performance Based Pathway | FDA